Stability of rock-filled mesh bags

Niels G. Jacobsen[1], Naika NA Barrera[2*], Clara Giarrusso[3*], and Erik D. Christensen[4]

[1]Vattenfall Vindkraft A/S, Ørestads Blvd 108, 2300 Copenhagen, Denmark. nielsgjoel.jacobsen@vattenfall.com
2 Orsted, Nesa Alle 1, 2820 Gentofte, Denmark. naika@orsted.com.
3 FORCE Technology, Hjortekærvej 99, 2800 Kgs. Lyngby, Denmark. cgi@forcetechnology.com
4Section of Fluid Mechanics, Coastal, and Maritime Engineering, DTU Construct, Technical University of Denmark, Koppels Allé, Bld. 403, 2800 Kgs. Lyngby, Denmark. edch@dtu.dk
[*]Both authors to be considered as second author.

ABSTRACT

Rock-filled mesh bags is an appealing method for both temporary and permanent stabilization in the offshore environment due to ease of installation, however, there is limited empirical evidence as to their performance which makes assessment of design safety factors challenging. The present work derives a critical mobility number for a singular rock-filled mesh bags far from any other infrastructure, and its expected failure mechanism: Sliding or over-turning. The critical mobility number is established through an experiment with individual rock-filled mesh bags in waves-only and current-only conditions, respectively. The rock-filled mesh bags are placed on both smooth and rough seabed. Engineering guidance is offered on how to extrapolate findings to the stability of the rock-filled mesh bags in (i) combined waves-and-current and (ii) in the proximity to offshore structures.

INTRODUCTION

Rock-filled mesh bags (RFMBs) are observed as an attractive solution for temporary and remedial works in the offshore wind sector, since they are relatively easy to install, and there is good control over impact energies on any stabilized object compared to loose rock installation. There is, however, a lack of information on the stability limit of the RFMBs which makes it challenging to quantify the suitability of RFMBs. Furthermore, since the stability limit is unknown it is also impossible to assess the remaining capacity in restraining subsea assets such as pipelines and submarine cables, or the functioning of RFMBs as scour protection. The latter application was investigated by Riezebos et al. (2022) where they identified the internal displacement of the filling material as a failure mechanism that may dislodge RFMBs from the grouped configuration. Once a single RFMB was dislodged, its movement across the otherwise stable RFMB scour protection was significant, and its movement could be a risk for e.g. cables and pipelines on top of the RFMB-based scour protections.

The lead author has seen some designs where empirical formulations were applied (e.g. the CIRIA C683 (2007), chap. 5.2.3); however, those design formulations are (i) exclusively intended for steady current and (ii) there is a number of design (tuning) parameters that opens for designs discussions on the quantitative accuracy for the offshore environment.

The lack of empirical evidence for the stability of RFMBs in the offshore environment motivated the present small-scale experimental campaign where the stability of 15 difference scaled RFMBs was investigated for waves-only and current-only, respectively. First, theoretical considerations as to a suitable non-dimensional mobility number is proposed for sliding and overturning failure of a single RFMB. Secondly, the experimental setup is described, followed by a presentation of the results, and a discussion on the unification of the current-only with the wave-only results. Discussions and conclusions are then presented.

THEORETICAL STABILITY CONSIDERATIONS

RFMBs can be subject to two different types of instability: sliding or overturning. Both will be considered here to derive a theoretical form of the mobility number. The sliding equilibrium reads (here assumed static, so encapsulated pore water can be ignored, which is not the case, when the RFMB moves):

$$\frac{1}{2}\rho_w A C_D |u| u + \rho_w V C_M \frac{\partial u}{\partial t} = \left(mg - V_r \rho_w g - \frac{1}{2}\rho_W A C_L u^2 \right) \mu_s \tag{1}$$

Here, ρ_w is the density of water, A is a frontal area of the RFMB, C_D is the coefficient for drag, u is the free-stream velocity, V is the volume of the RFMB (assuming contained water to be effectively trapped in the pores), C_M is the inertia coefficient, t is time, $m = V_r \rho_s$ is the dry mass of the RFMB, V_r is the volume of solid particles, ρ_s is the density of the solid particles, g is the acceleration due to gravity, C_L is the lift coefficient, and μ_s is the friction factor between RFMB and the seabed. The left-hand side of Eq. (1) describes the destabilizing inline forces while the right-hand side gives the stabilizing force from friction due to the mass corrected for buoyancy and hydrodynamic lift. In the following, a simple stability number covering both the steady current and wave cases are adopted, so it is assumed that inertia forces are much smaller than drag forces. Rearranging, the stability limit reads as follows at maximum velocity $u = u_m$:

$$\Psi_n = \frac{u_m^2}{(1-n)(s-1)gD} = \alpha \frac{2\mu_s}{C_D + \mu_s C_L} \tag{2}$$

Here, Ψ_n is the porosity corrected mobility number, $s = \rho_s / \rho_w$ is the relative density, it is utilized that $V_r = (1-n)V$, n is the porosity of the filling material, and $D = \alpha V / A$ is the diameter of the RFMB. All four parameters on the right-hand side are unknown, so an experimental campaign is proposed to identify the critical mobility limits for RFMB under waves and currents. $\Psi = \Psi_\mathrm{n}(1-n)$ is defined and applied throughout below.

The equilibrium in Eq. (1) is due to sliding, while the following equilibrium describes the overturning stability of the RFMB (again applying $C_M = 0$ and evaluated for $u = u_m$):

$$\frac{1}{2}\rho_w A\left(C_D\frac{H_b}{2}+C_L\frac{D}{2}\right)u_m^2=(mg-V_r\rho_w g)\frac{D}{2} \quad (3)$$

H_b is the representative height of the RFMB. Rewriting, the following stability criterion arises:

$$\Psi_n=\frac{u_m^2}{(1-n)(s-1)gD}=\frac{2\alpha}{C_D\,H_b/D+C_L} \quad \text{with} \quad \Psi=(1-n)\Psi_n \quad (4)$$

This is the same mobility number as in Eq. (2); however, the right-hand side differs with a reduced importance of inline drag compared to sliding stability: for RFMBs $H_b/D\simeq 0.1-0.2$. Since the nominators on right-hand side in Eqs. (2) and (4) are roughly the same with μ_s in the order of unity, it is expected that sliding instability will occur when seabed roughness can be overcome. Only, when the RFMB is placed on a (very) rough surface, overturning of the RFMB will take place. There is no practical difference between Ψ_n and Ψ given the small range of n in the experimental campaign (see Table 1), so presentation of results is limited to Ψ which is easier to work with from a practical engineering perspective. Omission of n in the design limits also eliminates the risk of designers using the porosity of the filling material as a tuning parameter to achieve a formally stable solution.

It is noted that the definition of the mobility numbers differs from the work by Antalion and Giarrusso (2022), so the quantitative limits are different. The present work is recommended for design.

EXPERIMENTAL CAMPAIGN

Testing facility

The experimental campaign was conducted in wave and current flumes at the Technical University of Denmark (Flumes 1 and 3). The flumes are approximately 35 m long, 0.8 m deep, and 0.6 m wide. Flume 1 was applied for wave-only tests and Flume 3 for current-only tests.

Figure 1: Scaled RFMBs (MD04 through MD06 left to right).

Scaled RFMBs and seabed preparation

The scaled RFMBs are listed with their properties in Table 1, where name, mass, density of filling material, porosity, diameter, and height are the main characteristics. The mass of the scaled RFMBs was measured at the start and end of the experimental campaign with insignificant loss of material. The LD (low density) and ND (normal density) are plastic particle and crushed rock material, respectively, while the MD materials are mixes of the LD and ND materials. The particle density and porosities were averaged over ten samples. Scaled RFMBs (MD- class) are shown in Figure 1.

Table 1: Overview of RFMB characteristics at start of experiments

Name	Short name	Mass [g]	Particle density [g/cm3]	Porosity [-]	Diameter [cm]	Height [cm]
LD01	LD	35.4	1.36	0.416	5.5	2.2
LD02		50.8			6.5	2.5
LD03		85.7			8.0	2.7
LD04		129			9.0	2.9
LD05		170			10.0	3.0
LD06		200			11.0	3.1
MD01	MD+	35.4	1.72	0.387	5.5	1.9
MD02		50.8			6.5	1.9
MD03		85.7			7.5	2.5
MD04	MD-	35.4	1.50	0.373	4.8	2.5
MD05		50.8			5.8	2.6
MD06		58.7			7.3	2.8
ND01	ND	35.4	2.45	0.387	5.0	1.8
ND02		50.8			6.0	2.0
ND03		58.7			7.0	2.2

Two seabed preparations were considered, namely a smooth concrete floor and a rock cover made of loose rocks with a median diameter of 5 mm. The cover thickness was 30 mm, and the rocks were sufficiently large to be immobile for all test conditions.

Test conditions

Waves were generated in water depths from 0.3 m to 0.5 m, with wave periods from 1.0 s to 2.5 s, and wave heights from 0.05 m to 0.15 m. A total of 46 wave conditions were investigated for the smooth seabed and 41 wave conditions for the rough seabed. All RFMBs were considered for both bed preparations resulting in 690 data points (smooth bed) and 615 data points (rough bed). The discharge in the case of current-only ranged from 16 l/s to 181 l/s with an achieved maximum depth-averaged current of 0.61 m/s.

Near-bed velocity

The discharge was measured in the flume as well as the water depth for the current-only case, which directly allowed for calculation of the depth-averaged velocity U_c.

In the case of waves-only, the velocity field was derived from the free surface elevation. The decomposition technique for nonlinear regular waves by Jacobsen et al. (2012) was employed on the measured surface elevation at the five wave gauges; a small modification was introduced by also considering the second-order free harmonic which was observed in the flume for highly nonlinear waves (small water depth and large wave height). The near-bed orbital velocity field was predicted based on second-order wave theory super-imposed for the incident and reflected wave fields, respectively, as well as the linear wave solution for the second-order free wave component. The maximum, absolute orbital velocity was applied in the evaluation of $KC = u_m T/D$ and Ψ. T is the regular wave period, and KC is the Keulegan-Carpenter number.

Identification of RFMB state

The state of the RFMBs was identified visually and the states differ between the waves-only and current-only cases. In the case of current-only, the RFMBs are either static or moving, however the approximate point of incipient motion will be assigned a separate classification. In the case of wave-only, three classes were identified: static, rocking, or sliding/rolling. Rocking is when slight movement of RFMB is observed without horizontal translation. Identification was made within the first 60 s of the wave field and stability in current-only was made for each steady current condition after change of the current speed.

RESULTS

Current-only conditions

The incipient motion of the RFMBs was found to differ between the type of seabed preparation. In the case of the smooth bed, all RFMBs were sliding while all RFMBs became unstable through overturning on the rough bed. This is already conceptually understood through theoretical considerations above, where static friction is expected to be largest for the rough seabed preparation and the importance of inline over lift decreases for overturning instability.

The mobility number Ψ is depicted as a function of the Reynold's number $Re = U_c D/\nu$ in Figure 2, and the critical value is approximately constant for each of the seabed preparations (smooth bed to the left and rough bed to the left). The steady, depth-averaged current U_c is applied in place of u_m in the evaluation of Ψ.

There is some scatter in Figure 2 and most noticeably for the rough seabed preparation, however, an empirical formulation for the critical mobility number for an RFMB is proposed as follows:

$$\Psi_{cr,c} = \frac{U_c^2}{(s-1)gD} = \begin{cases} 0.40 \pm 0.10 & \text{for smooth bed} \\ 0.51 \pm 0.06 & \text{for rough bed} \end{cases} \quad (5)$$

It is furthermore seen that the similar non-dimensional critical limit is found for all model RFMBs irrespective of the density of the filling material (see Table 1). A prominent source of experimental error is likely the fact that it is hard to increase the discharge in small steps, and a discharge increase of 10% results in a 20% increase in Ψ. Given the spread and the inherent uncertainty given the accuracy of the discharge increments, it is proposed to apply lower-bound limits: $\Psi_{cr,c} = 0.40 - 0.10 = 0.30$ for a smooth bed, and $\Psi_{cr,c} = 0.51 - 0.06 = 0.45$ for a rough bed.

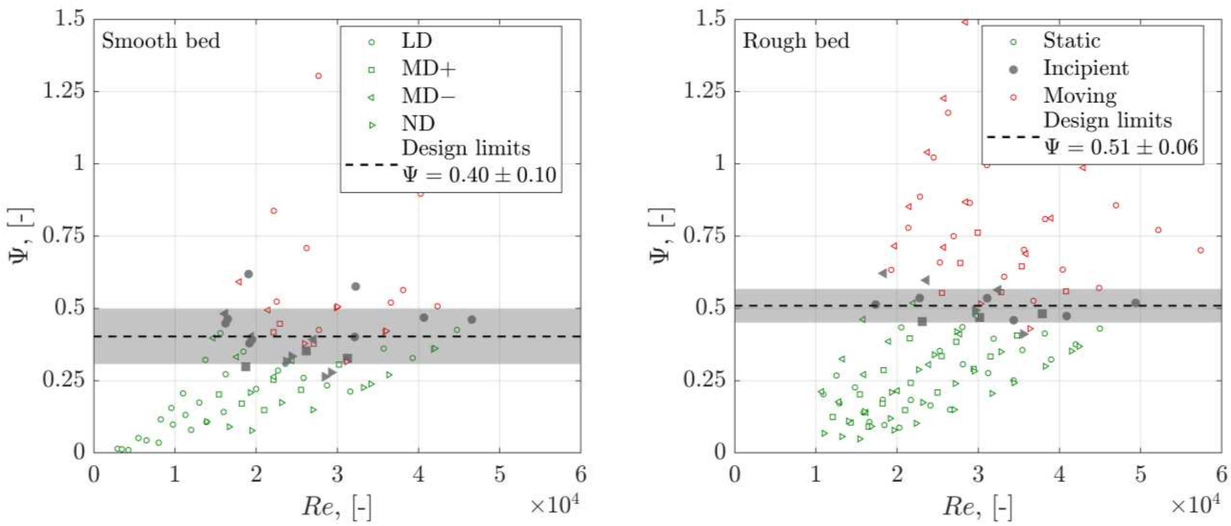

Figure 2: The stability diagram $\Psi(Re)$ in the case of a steady current for smooth (left) and rough (right) seabed.

Wave-only conditions

The stability diagram for $\Psi(KC)$ for waves-only is depicted in Figure 3 and a reasonable division between the static and rocking/moving RFMBs is observed, while there is a considerable overlap between the rocking and moving classifications. However, this is of minor importance from a practical engineering perspective, so it is possible to propose a stability limit for static RFMBs based on the available data sets. It is proposed as follows:

$$\Psi_{cr,w} = \frac{U_m^2}{(s-1)gD} = \begin{cases} \max(0.013KC, 0.04) & \text{for smooth bed} \\ \max(0.015KC, 0.06) & \text{for rough bed} \end{cases} \quad \text{for} \quad KC < 15 \qquad (6)$$

The lower limit is introduced to consider a lower threshold of motion. It was investigated to use a mobility number based on an assumption of inertia-dominated forces for small KC (assuming $C_M \neq 0$, $C_D = C_L = 0$ in Eq. (1)), however, this was inconclusive, and further analysis is left for future work. The stability limit in Eq. (6) is valid for $KC < 15$. Eq (6) is proposed based on the consideration that any instability of RFMBs is unwanted, while some conservatism in the critical mobility number is accepted. Consequently, the design limit is proposed such that most of the rocking and moving classifications fall above of the design limit for $KC > 8$. The limit of $KC > 8$

is used as a practical lower limit for RFMBs in the offshore environment. Inserting KC in Eq. (6) and isolating the critical near-bed velocity results in the following simple expression:

$$U_{m,cr} = \alpha T(s-1)g \quad \text{for} \quad KC < 15 \tag{7}$$

Here, $\alpha = 0.013$ for smooth beds and $\alpha = 0.015$ for rough beds.

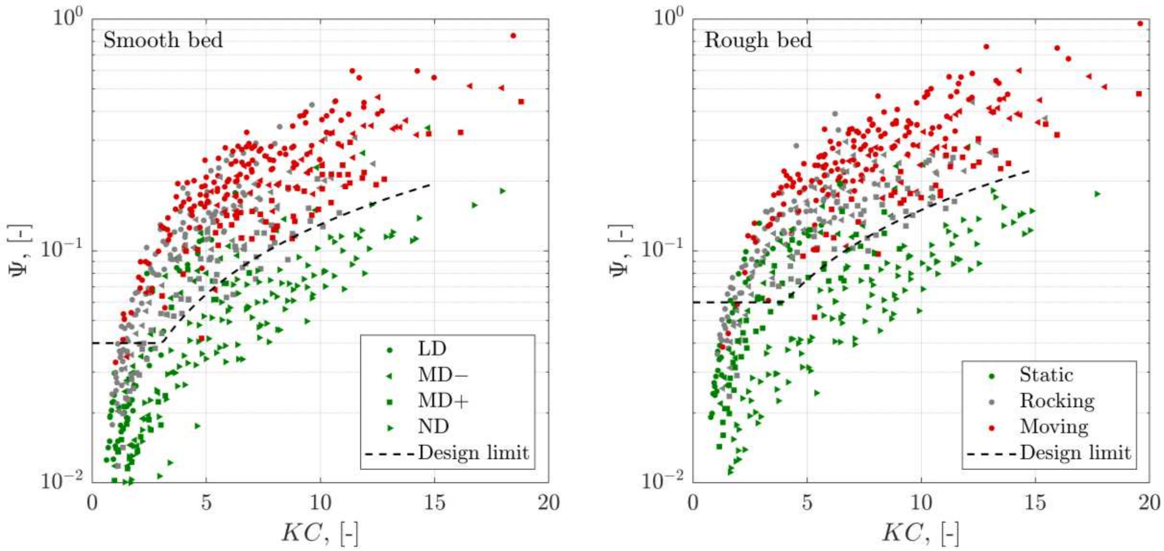

Figure 3: The stability diagram $\Psi(KC)$ for waves-only in the case of a smooth (left) and rough (right) seabed.

The scatter in the stability classifications means that not all points are on the correct side of the design limit. The degree of accuracy is summarized in Table 2, where the percentage correct and in-correct classification is summarized. The state of rocking and moving is captured with a high degree of accuracy for all data points and even better for $KC > 8$ (see Table 3).

Table 2: Overview of the correct and incorrect classification for smooth and rough beds. Given in percentages (left columns) and absolute numbers (right columns). All data points.

Classification	Smooth bed				Rough bed			
	Correct		Incorrect		Correct		Incorrect	
Static	85.6%	231	14.4%	39	76.7%	181	23.3%	55
Rocking	77.5%	155	22.5%	45	82.1%	142	17.9%	31
Moving	96.4%	212	3.6%	8	97.6%	201	2.4%	5

Table 3: As in Table 2. For data points with $KC > 8$.

Classification	Smooth bed				Rough bed			
	Correct		Incorrect		Correct		Incorrect	
Static	88.2%	45	11.8%	6	86.9%	53	13.1%	8
Rocking	92.3%	24	7.7%	2	87.5%	5	12.5%	5
Moving	98.9%	88	1.1%	1	99.1%	106	0.9%	1

Linking current and wave-only critical mobility limits

The critical mobility limit for the current-only case is based on the depth-averaged current U_c, while the RFMBs experience the local current velocity in close proximity to the bed. The near-bed velocity was estimated at top of the RFMBs based on the 1/7-power law velocity profile which resulted in local velocities in the range of $(0.7 - 0.78)U_c$. Applying the same reasoning as above, the updated lower critical mobility limit for RFMBs becomes 0.16 for a smooth bed and 0.24 for a rough bed based on a near-bed current speed. These limits are reached at $KC = 12.5$ and 16.2 for smooth and rough beds in the wave-only case, respectively. These are KC-values at the edge of empirical validity for the wave-only results, so it is left unconcluded if the design limits of 0.16 and 0.24 can be considered as the value towards which $\Psi_{\text{cr,w}}$ converges for large KC. It is recommended that these values are conservatively adopted as upper critical mobility limits.

DISCUSSION AND FUTURE WORK

Comparison with manufacturers' critical velocity limits

A couple of values for the proposed mobility number were identified from manufacturers' publicly available documentation, and their values are plotted together with the current-only design limits in Figure 4 (left panel), and with wave-only design limits for a period range of 9-13 s (right panel). This suggests that the manufacturers' stability limits are reasonable design values for a rough seabed and a steady current, but critical velocities published by manufacturers are non-conservative in waves and thus not applicable for use in the offshore environment.

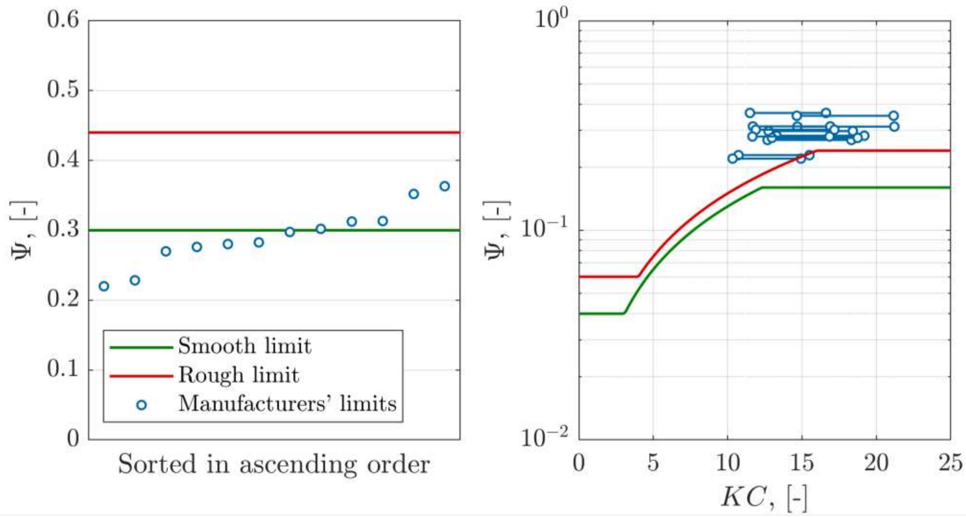

Figure 4: Comparison between empirical current-only (left) and wave-only (right) stability limits and mobility numbers from undisclosed manufacturers. Wave periods for 9-13 s used for KC number.

Application of the design limits

The proposed design limits for RFMBs are based on a small-scale laboratory experiment in the absence of any disturbance, e.g. monopile or jacket foundations. Consequently, should the design limits be applied for RFMBs adjacent to a foundation, an appropriate account should be made of the flow disturbance by the foundation. For monopile foundations, the potential flow solution (Sumer and Fredsøe, 1999, IEC-61400:3) will in most cases be sufficiently accurate, though if the RFMB is installed on a thick scour protection, additional flow amplification effects shall be accounted for. Secondly, local turbulence due to wakes and horseshoe vortex ought to be considered, but there is limited practical guidance on this. In any case, the mobility number should be evaluated based on the expected maximum design wave height in a given wave field, since displacement of RFMBs are driven by instantaneous failure.

Most offshore design conditions are combinations of waves-and-current, which was not covered in the present experimental study. A first extrapolation could be to estimate the instantaneous critical velocity as $u_m + U_c$ (or any other representative current velocity) and apply Eq. (6) in combination with the upper critical mobility limits of 0.16 (smooth bed) and 0.24 (rough bed). Here, $KC_{wc} \equiv (U_m + U_c)T/D$ should be applied in place of KC.

It is furthermore stressed that the present design limits do not account for any additional loading on the RFMB which will originate from the offshore asset that the RFMB is installed on top of or adjacent to. The combined loading on and stability of a RFMB in such a situation requires a description of the force coefficients for RFMBs. This can be obtained from simultaneous measurements of the forces and the local velocity field.

Finally, it is recommended that the rough seabed limits are applied when the RFMB is installed on top of a scour protection, while it is proposed to apply the smooth seabed limits, if the RFMB is installed directly on the seabed or on top of concrete mattresses for stabilization over e.g. cables and pipelines at crossings. It is acknowledged that concrete mattresses are somewhat rough, however, for the sake of conservatism, they could be considered smooth until experimental works or field observations conclude otherwise.

Future work

One of the constraints of the present work was that the ND RFMBs were stable under all wave conditions, so there could potentially be a scaling effect not captured in the non-dimensional quantities. However, given the similar stability limits for all densities for a steady current, it is claimed that the density of the rock fill has a minor impact. Nonetheless, future verification of the design limits with a larger scale factor and possibly with ND and high density (HD) filling material would be welcomed as this eliminates the need for engineering interpretation. It would also be useful to apply an experimental facility where the transition from wave-dominated to current-dominated conditions can be investigated.

The present work did not include near-bed velocity measurements and synchronization between the incipient motion and the instantaneous velocity field. This means that it was not possible to determine whether there is an inertia-dominated and a drag-dominated regime in waves-only, albeit likely. It is recommended to investigate this in future studies.

While the present work focused on regular waves, it is still unknown whether individual extreme waves or wave grouping in an irregular wave field is sufficient to displace the RFMB, so a repetition of the present work for irregular waves is recommended.

RFMBs are often applied near offshore structures which change the flow field and introduces wake-induced turbulence. While engineering guidance is provided above, it would be beneficial to derive empirical stability criteria for RFMBs under these adverse conditions. Finally, RFMBs are applied for temporary and permanent stabilization of offshore assets (e.g. pipelines and submarine cables), so it is important to analyze the stabilizing capacity of the RFMB when subject to drag and lift: Can the RFMB pull the offshore asset along the seabed? Can the hydrodynamic load on the asset become so large that it is pulled out from underneath the RFMB? Both scenarios are unwanted and should be mitigated.

CONCLUSION

An empirical stability limit for an individual rock-filled mesh bags (RFMB) was proposed in the present work for RFMBs placed on either smooth or rough seabed. The stability limits were proposed based on steady current-only and waves-only hydrodynamic loading, respectively, and the current-only tests suggest an upper critical mobility limit to be applied in case of wave-dominated environments at large KC (see e.g. Figure 4, right panel). Engineering guidance was provided on how to account for the proximity of offshore structures, combined waves-and-current loading conditions, and when to apply the smooth and rough design limits. The hydrodynamic reduction in restraining capacity of an RFMB on e.g. pipelines and cables is left for future experimental investigations.

REFERENCES

Antalion, N. and Giarrusso, C. (2022). Stability of rock bags for scour protection. Master thesis, Technical University of Denmark, December.

CIRIA C683 (2007). The Rock Manual: The Use of rock in hydraulic engineering. 2nd edition. Published by CIRIA, London.

IEC 61400:3 (2019). *Wind energy generation systems – Part 3:1: Design requirements for fixed offshore wind turbines*. International Electrotechnical Commission.

Jacobsen, NG, Fuhrman, DR, and Fredsøe, J. (2012). A wave generation toolbox for the open-source CFD library: OpenFoam®. *International Journal for Numerical Methods in Fluids*, **70**(9), 1073-1088.

Riezebos, HJ, Van Velzen, Bruinsma, N., Jacobsen, NG, and Waßmuth, S. (2021). Scaling and performance of a flexible mesh bag scour protection. *In proceedings for the 10th International Conference on Scour and Erosion*. 10 pages.

Sumer, BM and Fredsøe, J. (1999). *Hydrodynamics around cylindrical structures*. World Scientific, Advanced Series on Ocean Engineering, Vol. 12, 1st edition, 2nd print.